Vinyl Acetate Synthesis on Homogeneous and Heterogeneous Pd-Based Catalysts: A Theoretical Analysis on the Reaction Mechanisms[#]

José J. Plata,[†] Mónica García-Mota,[†] Ataualpa A. C. Braga,[†] Núria López,*[,†] and Feliu Maseras*[,†,‡]

Institute of Chemical Research of Catalonia (ICIQ), Avgda. Països Catalans, 16, 43007 Tarragona, Catalonia, Spain, and Departament de Química, Universitat Autònoma de Barcelona, 08193 Bellaterra, Catalonia, Spain

Received: March 31, 2009; Revised Manuscript Received: August 17, 2009

Vinyl acetate can be synthetized by both homogeneous and heterogeneous processes involving Pd atoms as reaction centers. We have determined the reaction mechanisms by means of density functional theory applied to molecular models for the homogeneous catalyst and to slabs that model the most active heterogeneous ensemble to unravel the similarities and differences in the reaction networks under these different conditions. We find that although the reaction network is similar, the rate determining step is different. Thus, direct extrapolations from organometallic chemistry to gas-phase heterogeneous catalysis should be handled with care.

Introduction

Vinyl acetate, VA, is an important monomer involved in the production of polymers employed as paints, adhesives, coatings, and fibers.[2] VA is synthetized from ethylene and acetic acid, and although initially the synthetic process was based on homogeneous palladium-catalysts,[3] now it has almost been completely substituted by Pd-based heterogeneous process.[4−7] The preference for the heterogeneous process is based on the better performance against corrosion and poisoning by chlorides and water. Both the homogeneous and the heterogeneous routes are reproduced in Figure 1, where the benzoquinone/hydroquinone (BQ/HQ) pair is used as external oxidant for the homogeneous reaction.

The homogeneous process was described by Moiseev around 1960,[3,8,9] and it belongs to the family of oxidative acyloxylation reactions.[10] Acyloxylations can be carried out in acetic acid at moderate temperatures (50−60 °C).[11] The mechanism shows the following steps.[12,13] First, the alkene coordinates to the Pd(II) catalyst. In the following step, the C−O bond is formed by nucleophilic addition of the acetate to the alkene. The next step is the C−H cleavage that results in formation of the C−C double bond. Finally, regeneration of the catalyst by a redox system takes place. The first description of the mechanism was developed by van Helden et al., who assumed that the elimination of the β-hydrogen atom was the rate limiting step.[14]

The industrial heterogeneous catalysts are based on silica suported Pd−Au alloys with excess of alkali acetate. The reaction takes place at 130−200 °C and 5−10 atm and the yield is 96% or higher of VA in terms of ethylene conversion.[4] Oxygen is employed in the reaction to drive acetic acid dehydrogenation, and it is released as water molecules. In the reaction mechanism oxygen is dissociated on the surface, then one of the oxygen atoms drives the dehydrogenation of acetate. Ethylene can be adsorbed in a neighboring Pd center and then

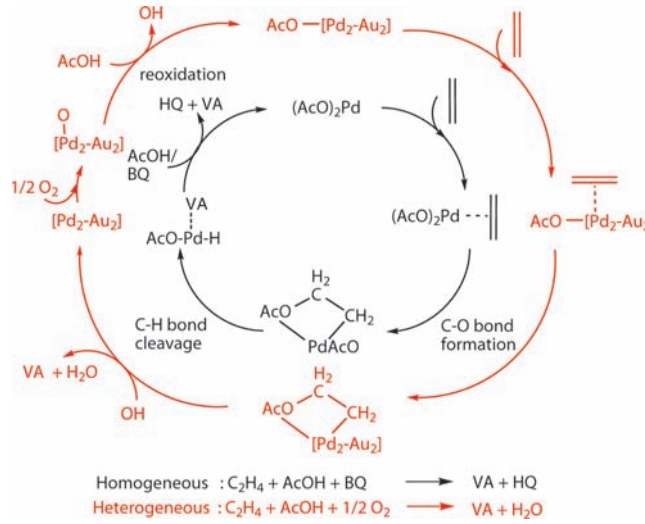

Figure 1. Reaction scheme for the synthesis of vinyl acetate from ethylene and acetic acid on Pd-based catalyst.

the C−O coupling takes place, finally an oxygen atom or a hydroxyl group can provoke the β-hydrogen elimination leading to the product. Detailed experimental studies exist on the ensemble effects found for VA synthesis over Pd−Au alloys.[15−19]

Since the same metal is employed in both homogeneous and heterogeneous versions of the catalyst, there is an interest to analyze the similarities and differences on the reaction mechanisms on both cases. Both homogeneous[20,21] and heterogeneous[22] catalysis have been intensely and successfully studied from a computational point of view, but seldom in direct comparison. In fact, the understanding of the link between homogeneous and heterogeneous catalysis constitutes a challenge in the development of new catalysts.[23,24] The present work follows our analysis for the selective activation of alkynes on gold catalyts.[25]

To this end, we have employed theoretical tools based on density functional theory (DFT). We considered for both systems the simple model reaction between ethylene and acetic acid.

[#] Part of the "Walter Thiel Festschrift".

* To whom correspondence should be addressed. E-mail: (N.L.) nlopez@iciq.es; (F.M.) fmaseras@iciq.es.
[†] Institute of Chemical Research of Catalonia (ICIQ).
[‡] Universitat Autònoma de Barcelona.

10.1021/jp902929x CCC: $40.75
Published on Web 09/21/2009

For the homogeneous system, the catalyst employed was [Pd(κ^2-$O_2CCH_3)_2$]. It has been suggested that the catalyst may act in a dimeric or trimeric form, but previous studies have shown the reaction to take place in a single palladium center;[26] the monomer should thus be a good model. This previous work by Kragten et al.[26] is to our knowledge the only previous computational study on the homogeneous process. It did consider the dimeric form of the catalyst in some steps, but it did not compute the full catalytic cycle, and it applied a very simplified model system in the calculation of the transition state for the only step that was analyzed in detail. The monomeric palladium acetate model has been also applied in the theoretical study of other reactions.[27] The oxidant in our study was *p*-benzoquinone, one of many that have been found to be experimentally efficient.[11] It is transformed in hydroquinone after the reaction. As for the heterogeneous system, the PdAu alloys form a continuous solid solution; on high gold composition range, Pd atoms can be prepared to be in the surface as impurities. It has been shown experimentally that the open (100) surface with a particular Pd dimer configuration (at a distance of $\sqrt{2}d_{Pd-Pd}$) is the most active for the reaction.[15]

Computational Methods

All calculations were performed at the DFT level. For the homogeneous reaction, we used the hybrid Becke3LYP[28−30] functional with a hybrid Becke exchange functional and a Lee−Yang−Parr correlation functional[28,29] as implemented in Gaussian03.[31] The Pd atom was described using an effective core potential for the inner electrons[32] and its associated double-ζ basis set for the outer ones. The 6-31G(d) basis set was used for the atoms H, C, and O.[33] Solvent effects were introduced in selected cases through PCM single-point calculations[34] on gas phase optimized geometries. Aniline was used as solvent due to its very similar dielectric constant compared to acetic acid ($\varepsilon_r = 6.89$ and 6.21, respectively). The structures of the reactants, intermediates, transition states, and products were fully optimized without any symmetry restriction. Transition states were identified by having one imaginary frequency in the Hessian matrix. The presented energies for the homogeneous processes correspond to potential energies corrected with zero-point energies and solvation effects. The relative gas phase potential energies with and without zero point energy corrections are collected in Table S1 (Supporting Information) and show no significant differences with the values discussed in the text. We decided against including entropic corrections because of the well-documented problems[35,36] for their accurate introduction for solvated systems through simple statistical thermodynamics based on gas phase calculations.

For the heterogeneous reaction, periodic density functional theory calculations have been performed with the VASP code.[37] A slab containing five layers represents the Au(100) surface with a p(4 × 4) reconstruction. Two of the surface Au atoms have been replaced by Pd reproducing the next-nearest neighbors local ensemble known to be the most active species.[15,25] The two outermost layers and the adsorbate degrees of freedom have been allowed to relax. The energies have been obtained within the RPBE[38] functional. Inner cores have been replaced by PAW[39,40] pseudopotentials while valence electrons have been expanded in plane waves with a cutoff energy of 400 eV. The Monkhorst-Pack scheme[41] with 2 × 2 × 1 k-points has been employed. Transition states have been located by the use of the climbing image version of the nudged elastic band algorithm[42] and in all cases a single imaginary frequency has been obtained for these structures.

The choice of the computational methods was based on the usual approaches currently applied in computational homogeneous and heterogeneous catalysis. The use of different descriptions can however hamper the comparison. In order to evaluate the effect of the use of the different computational set-ups, we carried out a systematic series of VASP RPBE single-point calculations on all the Gaussian03 B3LYP optimized structures for the homogeneous systems. A cubic box of 15 $Å^3$ was used in these periodic calculations. The results, collected in Table S2 (Supporting Information), show relative potential energy differences of 36 kJ/mol at most, and in no case modify the qualitative analysis of energetics discussed in the text.

Complete Reaction Paths

The key features of the reaction mechanisms have been previously characterized computationally with some degree of detail for both the homogeneous[26] and heterogeneous counterpart.[43,44] However, to our knowledge, a comparison of the full catalytic cycles had not been previously reported. We carried out this calculation, and the overall profile for the reaction is presented in Figure 2 where both reaction mechanisms have been overlapped. We find both reaction mechanisms to have the three main steps that were expected, ethylene-acetate coupling (C−O formation), β-hydrogen elimination, and catalyst reoxidation. The nature of the rate-determining step is however different and the exothermicity of the reaction, due to the presence of the oxygen-water pair, is much larger for the heterogeneous process.

For the homogeneous system, the barriers for the three main steps are 74.9, 96.2, and 92.1 kJ/mol, respectively. The rate-determining step involves therefore the β-hydrogen transfer in agreement with previous experimental considerations.[14] For the heterogeneous counterpart the reaction shows a major reaction bottleneck (127.4 kJ/mol) associated to the formation of the C−O bond on the surface. Hydrogen activations are relatively easy both for acetic acid and the hydrogenated VA product. The main steps for the reaction are thus very similar, but the relative barriers are different. We will analyze in what follows in more detail each of the main three steps.

Ethylene-Acetate Coupling

In the homogeneous reaction, the ethylene-acetate coupling consists in the formal insertion of the ethylene into one of the Pd−O bonds of [Pd(κ^2-$O_2CCH_3)_2$], see Figure 3a. The κ symbol indicates that the ligand only coordinates the metallic center by two of the three possible atoms, in this case the two O atoms. In the starting point of this step, the ethylene is coordinated η^2 to the metal, and one of the acetates is coordinated in a κ^1_O mode with Pd−O distances of 2.202 and 2.772 Å; see hoI1. The presence of the ethylene distorts thus strongly the initial κ^2 coordination of one of the acetates in the catalyst, although this involves no insertion yet into the Pd−O bond. The insertion takes place at the transition state where a rotation takes place of both the acetate and ethylene fragments. The barrier to reach this structure is 74.9 kJ/mol, and the C−O distance is 2.163 Å. In the final state, the hydrogenated VA, VAH, is bound to the metal center by the terminal C and O atoms. The newly formed C−O distance is 1.471 and the metal-to-carbon and metal-to-oxygen distances are 2.013 and 2.085 Å, respectively. The step is mildly exothermic with the final state 6.7 kJ/mol below the initial state. This is not the rate determining step for the whole process, but the barrier of 74.9 kJ/mol is not neglectable, as had been considered in the previous computational study by

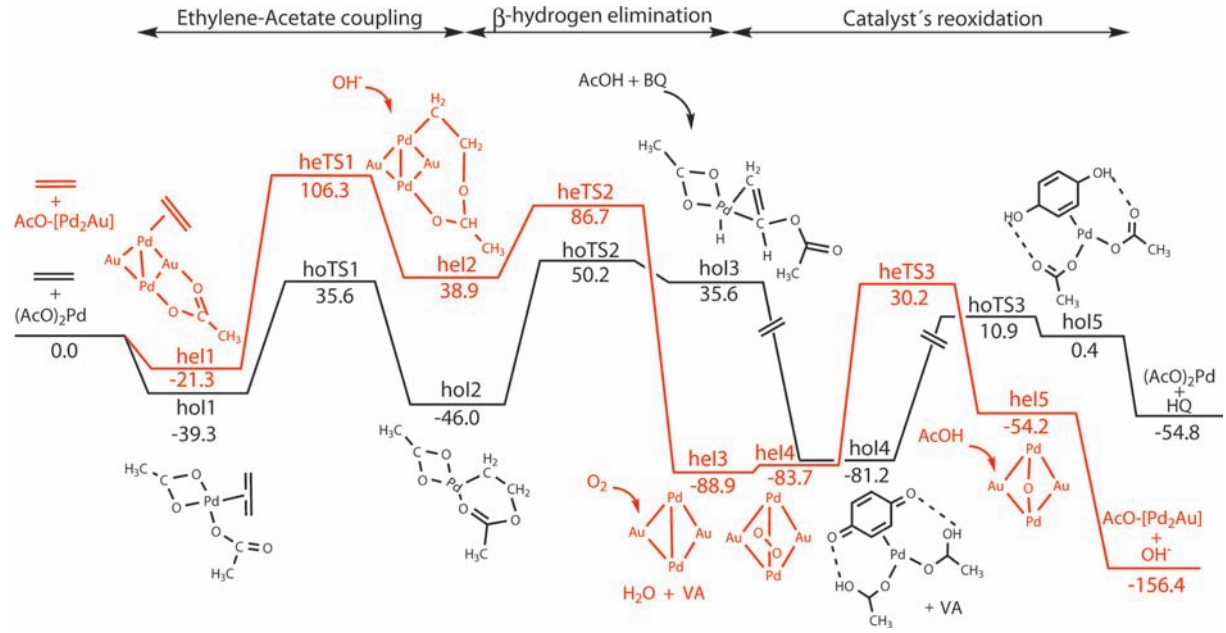

Figure 2. Energy profile for VA synthesis on the most active dimer of the PdAu(100) surface and with the homogeneous Pd^{2+} complex. The energies are in kilojoules/mole. Origin of energies is in both cases the metal acetate complex plus ethylene.

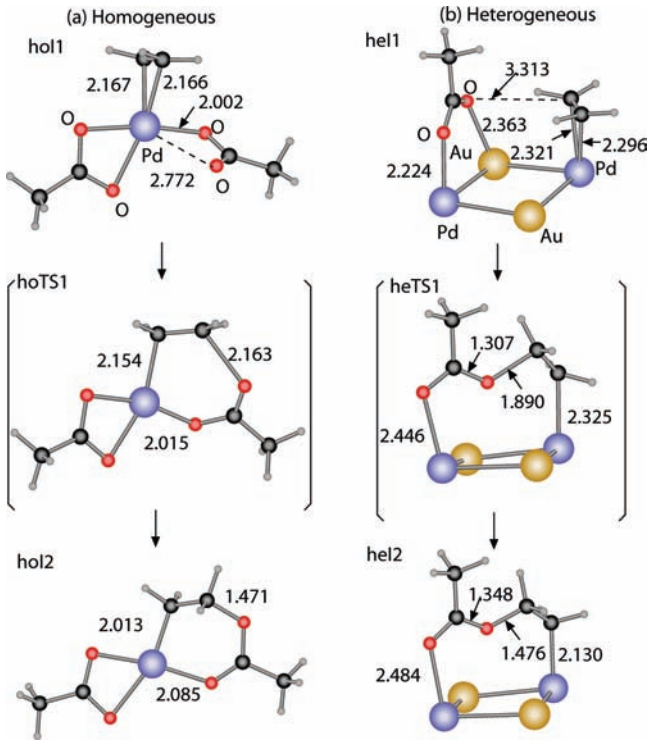

Figure 3. Initial, transition and final states for the formation of the C−O bond in (a) homogeneous catalyst; (b) heterogeneous catalyst.

Kragten et al.,[26] that had focused only in the barrier for the β-hydrogen elimination step.

On the heterogeneous process, in the initial structure ethylene and acetate are placed on different Pd atoms on the surface. Acetate shows a κ^1_O bonding configuration while ethylene is adsorbed in a π-Pd mode; see Figure 3 structure heI1. The initial C−O distance is 3.313 Å. The transition state is reached by a rotation of both reactants so that they face each other; the C−O distance at this point is 1.890 Å. In the final state, the terminal C and O atoms are bound to the active Pd centers on the surface and the new C−O bond distance is 1.476 Å. The final structure is more unstable than reactants by 60.2 kJ/mol, being the barrier 127.6 kJ/mol.

According to these results and even if the number of metal centers in the systems is different, the similarities in the initial and final states are important. The differences in the transition state structure can be linked to the Hammond−Leffler postulate[45,46] indicating that in the homogeneous case the C−O coupling is a reactant-like structure (due to the exothermicity of the reaction) while for the heterogeneous case a product-like transition state is obtained (i.e., the reaction is endothermic).

The barrier is significantly higher for the heterogeneous process. This is likely because the participation of two different metal centers stabilizes mainly the initial state thus discouraging the reaction from taking place.

***β*-Hydrogen Elimination.** β-Hydrogen elimination takes place from two different situations. In the homogeneous process, this step consists simply of the transfer of the β-hydrogen to the metal in the intermediate resulting from the C−O bond formation step; see Figure 4 structure hoI2. In the transition state, the hydrogen transfer is almost complete; Pd−H is 1.588 Å (to be compared with 1.535 Å in palladium-hydride) and C−H is 1.615 Å. This is consistent with the high endothermicity of the process. This step is endothermic by 81.6 kJ/mol, and the transition state is quite high in energy, 96.2 kJ/mol, and similar to the product. The relatively high barrier that makes this the rate-determining step is associated to the low stability of the palladium hydride complex. This barrier is very close to the value of 95 kJ/mol computed by Kragten et al. with a simplified model for the transition state.[26]

We explored also an alternative pathway where the hydrogen would not go to the palladium but to an external acceptor, which we introduced in the form of acetic acid. The energy for the transition state was higher by 13.8 kJ/mol, and we thus discarded this alternative pathway. This alternative pathway had been found to be favored in the previous work by Kragten et al., where it was labeled "outer sphere".[26] We think that the alternative pathway was heavily favored in the previous report because of the introduction of a free acetate anion without taking into account its lower abundance in the experimental glacial acetic acid conditions. The lower concentration of acetate with

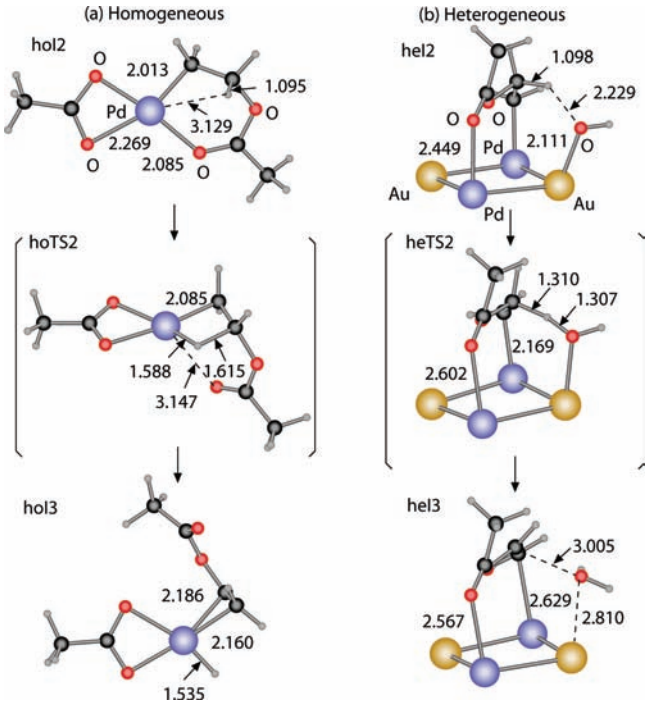

Figure 4. Initial, transition, and final states involved in β-hydrogen elimination. (a) Homogeneous catalyst, (b) heterogeneous catalyst.

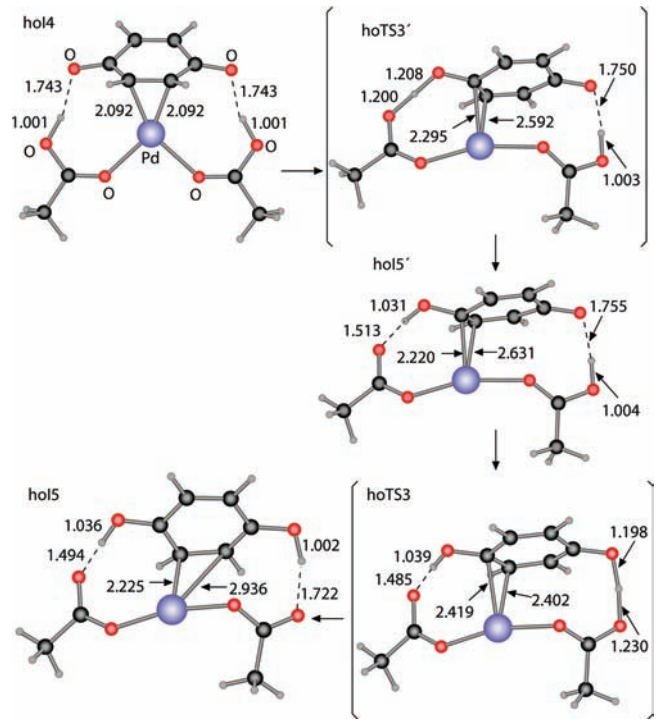

Figure 5. Key species involved in reoxidation of the homogeneous catalyst.

respect to acetic acid should affect the relative apparent rate constant, and the mechanism would be competitive at best with the one reported here. Moreover, if the previously reported value of 67 kJ/mol were correct, this would not be the rate determining step, which is in disagreement with the experimental observation.[14]

For the heterogeneous counterpart either oxygen or hydroxyl groups on the surface act as acceptors for the β-hydrogen atom; see Figure 4 structure heI2. In the initial state structure, VAH is adsorbed on the Pd centers through a $\kappa^2_{O,C}$ configuration. OH atoms can be adsorbed on Au atoms in the neighboring region. In the initial state, the distance between the β-hydrogen and the oxygen atom in the hydroxyl group is 2.229 Å. At the transition state, the proton is close to the hydroxyl group, 1.307 Å, and finally it evolves toward the formation of a water molecule. The basicity of hydroxyl groups on Au centers is known to be large and therefore the process takes place very easily.[47] The calculated barrier is 47.8 kJ/mol and both products readily leave the surface.

The main difference in this step is thus the nature of the proton acceptor. While for the homogeneous case the metal center acts as an inefficient acceptor, the availability of oxygen or hydroxyl species facilitates this particular reaction step in the heterogeneous process.

Catalyst Reoxidation

The reoxidation of the catalyst is done through different mechanism depending on the nature of the catalyst.

For the homogeneous version of the catalyst an external redox pair is needed.[3] In the present case, the benzoquinone-hydrobenzoquinone pair has been considered. The reoxidation does not take place directly from the final state of the previous step, the hoI3 complex, where a hydride coordinates to palladium. The reacting system must undergo some changes. First, a benzoquinone coordinates in an η^2 shape to palladium, resulting in a spontaneous movement of the hydride from palladium to the coordinated acetate, that becomes thus a κ^1 coordinated acetic acid. Next, a second acetic acid unit must come into the coordinating sphere of the metal and replace the vinyl acetate product, which is released. The rearrangements result in a complex, hoI4, where two acetic acids are coordinated κ^1 to the metal and the benzoquinone is coordinated in an η^2 shape. These steps, preliminary to catalyst reoxidation, are mechanistically complex and involve low barriers. Because of this they are not discussed in detail here, but collected in the Supporting Information, where three consecutive intermediates between hoI3 and hoI4 are presented. The highest energy transition state in this process is less than 5 kJ/mol above hoI3.

From this complex, the reoxidation takes place in two steps, shown in Figure 5. Each step consists of a hydrogen transfer from one acetic acid to the benzoquinone. The corresponding transition states have the expected shape with the hydrogen near the midpoint between the two oxygen centers involved. The O−H distances are 1.200, 1.208 Å in the first transition state and 1.230, 1.198 Å in the second. The energy of the transition states with respect to the starting point are 81.2 and 92.1 kJ/mol. Therefore, despite the complexity of the process, the barrier is still lower than for the β-hydrogen elimination. Thus, catalyst reoxidation is not the rate-determining step in the homogeneous process.

In the heterogeneous version of the catalyst, the surface can adsorb O_2; see Figure 6 structure heI4. The binding of O_2 molecular precursor is slightly endothermic by 5.2 kJ/mol and the O−O distance is 1.299 Å. The precursor is bonded to a Pd atom on the surface and the second O atom is facing a Au (thus similar to a bridge site). At the transition state, the O−O distance is elongated to 1.880 Å, and in the final state both O atoms are placed on different hollow sites on the surface. The transition state structure is higher than reactants by about 113.9 kJ/mol, thus reoxidation of the surface is not very easy due to the presence of Au on the surface. Once completed, reoxidation leads to two oxygen atoms on the surface which bear almost no magnetic moment. The final state is 29.5 kJ/mol higher in energy than the molecular adsorbed state.

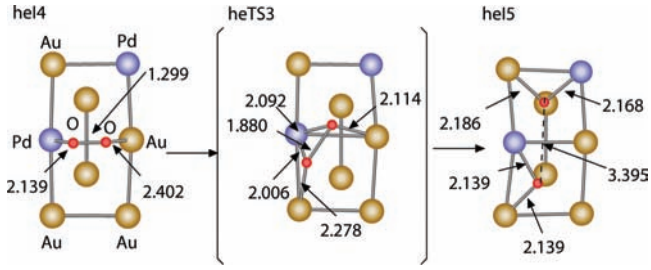

Figure 6. Initial, transition, and final states involved in reoxidation of the heterogeneous catalyst.

In this step the qualitative differences between the homogeneous and heterogeneous processes are the most significative. At least two steps are needed for the homogeneous process with the participation of the oxidant and those reactions are not directly transferable to the heterogeneous counterpart. However, these qualitative differences have little effect on the efficiency of the overall catalytic process, because reoxidation is never the rate-determining step.

Conclusions

The reaction mechanisms on both homogeneous and heterogeneous catalysis for the synthesis of vinyl acetate from ethylene and acetic acid contain the same steps. However, the thermochemistry for the complete process depends on the nature of the oxidant employed, and the rate determining steps in both cases are different. For the homogeneous catalysts the most demanding step is C−H cleavage while for the heterogeneous catalyst the C−O coupling is found to be the rate determining step in agreement with the experiments. The reoxidation process is far simpler in the heterogeneous situation, but it is in no case the rate-determining step. The complexity of reoxidation in the homogeneous case may be related to the generation of nanoparticles Pd(0) that has been found to compromise the selectivity toward the product.

Finally, the reaction takes place at lower temperatures in the homogeneous case than in the heterogeneous version of the catalyst (i.e., 50−60 °C to be compared with 130−200 °C). This agrees very well with the calculated barriers for the rate determining step that are significantly higher in the heterogeneous version of the catalyst (i.e., 127 vs 96 kJ/mol for the homogeneous case). This is similar to the results for the C−C coupling in homogeneous and heterogeneous Au catalysts,[25] where organometallic compounds are able to work under softer temperature conditions.

In conclusion, we demonstrate how homogeneous and heterogeneous processes in the case of VA synthesis are closely linked. However, the direct extension of one of the process to its counterpart is not straightforward since differences in the rate determining step might be strongly dependent on the nature of the catalyst.

Acknowledgment. We thank the ICIQ foundation, MICINN (Consolider Ingenio 2010 CSD2006-003, CTQ2006-00464BQU, CTQ2008-06866-CO2-02/BQU), GenCat (Grants 2009SGR0259 and XRQTC), RES, and CESCA for funding support and computational resources. J.J.P. thanks the ICIQ foundation for a Summer fellowship.

Supporting Information Available: Full reference for Gaussian03 program, additional energy tables, and Cartesian coordinates for all optimized structures with total energies. This material is available free of charge via the Internet at http://pubs.acs.org.

References and Notes

(1) Cordeiro, C. F.; Petrocelli, F. P. *Vinyl Acetate Polymers.* In Kirk-Othmer Encyclopedia of Chemical Technology, 5th ed.; Wiley: New York, 2005, Vol. 25, pp 557−591.
(2) http://www.vinylacetate.org/what.shtml, accessed February 23, 2009.
(3) Moiseev, I. I.; Vargaftik, M. N.; Syrkin, J. K. *Dok. Akad. Nauk SSSR* **1960**, *133*, 377–380.
(4) Bissot, T. U.S. Patent 4,048,096, 1977.
(5) Nakamura, S.; Yasui, T. *J. Catal.* **1970**, *17*, 366.
(6) Samanos, B.; Boutry, P.; Montarna., R. *J. Catal.* **1971**, *23*, 19.
(7) Nakamura, S.; Yasui, T. *J. Catal.* **1971**, *23*, 315.
(8) Smidt, J.; Sedlmeier, J.; Hafner, W.; Sieber, R.; Sabel, A.; Jira, R. *Angew. Chem., Int. Ed. Engl.* **1962**, *74*, 93.
(9) Smidt, J.; Hafner, W.; Jira, R.; Sedlmeier, J.; Sieber, R.; Ruttinger, R.; Kojer, H. *Angew. Chem., Int. Ed. Engl.* **1959**, *71*, 176–182.
(10) Goossen, L. J.; Rodríguez, N.; Goossen, K. *Angew. Chem., Int. Ed.* **2008**, *47*, 3100–3120.
(11) Beccalli, E. M.; Broggini, G.; Martinelli, M.; Sottocornola, S. *Chem. Rev.* **2007**, *107*, 5318–5365.
(12) Grennberg, H.; Simon, V.; Bäckvall, J. E. *J. Chem. Soc., Chem. Commun.* **1994**, 265–266.
(13) Grennberg, H.; Bäckvall, J. *Chem.−Eur. J.* **1998**, *4*, 1083–1089.
(14) van Helden, R.; Kohll, C. F.; Medema, D.; Verberg, G.; Jonkhoff, T. *Rec. Trav. Chim. Pays-Bas* **1968**, *87*, 961–962.
(15) Chen, M.; Kumar, D.; Yi, C.; Goodman, D. *Science* **2005**, *310*, 291–293.
(16) Chen, M. S.; Luo, K.; Wei, T.; Yan, Z.; Kumar, D.; Yi, C. W.; Goodman, D. W. *Catal. Today* **2006**, *117*, 37–45.
(17) Han, P.; Axnanda, S.; Lyubinetsky, I.; Goodman, D. W. *J. Am. Chem. Soc.* **2007**, *129*, 14355–14361.
(18) Wei, T.; Wang, J.; Goodman, D. W. *J. Phys. Chem. C* **2007**, *111*, 8781–8788.
(19) Kumar, D.; Chen, M. S.; Goodman, D. W. *Catal. Today* **2007**, *123*, 77–85.
(20) Vyboishchikov, S. F.; Bühl, M.; Thiel, W. *Chem.−Eur. J.* **2002**, *8*, 3962–3975.
(21) Ujaque, G.; Maseras, F. *Struct. Bonding (Berlin)* **2004**, *112*, 117–149.
(22) Nørskov, J. K.; Bligaard, T.; Hvolbaek, B.; Abild-Pedersen, F.; Chorkendorff, I.; Christensen, C. H. *Chem. Soc. Rev.* **2008**, *37*, 2163–2171.
(23) Somorjai, G. A.; Contreras, A. M.; Montano, M.; Rioux, R. M. *Proc. Natl. Acad. Sci. U.S.A.* **2006**, *103*, 10577–10583.
(24) Motta, A.; Fragala, I. L.; Marks, T. J. *J. Am. Chem. Soc.* **2008**, *130*, 16533–16546.
(25) García-Mota, M.; Cabello, N.; Maseras, F.; Echavarren, A. M.; Perez-Ramirez, J.; López, N. *ChemPhysChem* **2008**, *9*, 1624–1629.
(26) Kragten, D.; van Santen, R.; Neurock, M.; Lerou, J. *J. Phys. Chem. A* **1999**, *103*, 2756–2765.
(27) Biswas, B.; Sugimoto, M.; Sakaki, S. *Organometallics* **2000**, *19*, 3895.
(28) Becke, A. D. *J. Chem. Phys.* **1993**, *98*, 5648.
(29) Lee, C.; Yang, W.; Parr, R. G. *Phys. Rev. B* **1988**, *37*, 785.
(30) Stephens, P. J.; Devlin, F. J.; Chabalowski, C. F.; Frisch, M. J. *J. Phys. Chem.* **1994**, *98*, 11623.
(31) Frisch, M. J. et al. *Gaussian 03*, revision C.02; Gaussian, Inc.: Wallingford, CT, 2004.
(32) Andrae, D.; Haussermann, U.; Dolg, M.; Stoll, H.; Preuss, H. *Theor. Chim. Acta* **1990**, *77*, 123.
(33) Francl, M. M.; Pietro, W. J.; Hehre, W. J.; Binkley, J. S.; Gordon, M. S.; Defrees, D. J.; Pople, J. A. *J. Chem. Phys.* **1982**, *77*, 3654.
(34) Miertus, S.; Scrocco, E.; Tomasi, J. *Chem. Phys.* **1981**, *55*, 117.
(35) Braga, A. A. C.; Ujaque, G.; Maseras, F. *Organometallics* **2006**, *25*, 3647–3658.
(36) Robiette, R.; Aggarwal, V. K.; Harvey, J. N. *J. Am. Chem. Soc.* **2007**, *129*, 15513–15525.
(37) Kresse, G.; Furthmüller, J. *Phys. Rev. B* **1996**, *54*, 11169–11186.
(38) Hammer, B.; Hansen, L.; Nørskov, J. *Phys. Rev. B* **1999**, *59*, 7413–7421.
(39) Blöchl, P. *Phys. Rev. B* **1994**, *50*, 17953–17979.
(40) Kresse, G.; Joubert, D. *Phys. Rev. B* **1999**, *59*, 1758–1775.
(41) Monkhorst, H. J.; Pack, J. D. *Phys. Rev. B* **1976**, *13*, 5188–5192.
(42) Henkelman, G.; Uberuaga, B.; Jonsson, H. *J. Chem. Phys.* **2000**, *113*, 9901–9904.
(43) García-Mota, M.; López, N. *J. Am. Chem. Soc.* **2008**, *130*, 14406.
(44) Yuan, D.; Gong, X.; Wu, R. *J. Phys. Chem. C* **2008**, *112*, 1539–1543.
(45) Leffler, J. E. *Science* **1953**, *117*, 340–341.
(46) Hammond, G. S. A. *J. Am. Chem. Soc.* **1955**, *77*, 334–338.
(47) López, N.; García-Mota, M.; Gómez-Diaz, J. *J. Phys. Chem. C* **2008**, *112*, 247–252.

JP902929X